LRIG1 Affects Clonogenicity but Not Metastatic Potential in Non–small Cell Lung Cancer Cell Lines

Samuel Kvarnbrink (samuel.kvarnbrink@umu.se)
Department of Radiation Sciences, Umeå University, Sweden https://orcid.org/0000-0001-9342-7625
Håkan Hedman
Umeå University, Radiation Sciences
Mikael Johansson
Umeå University, Radiation Sciences

Research article

Keywords: leucine-rich repeats and immunoglobulin-like domains protein 1 (LRIG1), chemosensitivity, radiosensitivity, clonogenicity

Posted Date: October 30th, 2020

DOI: https://doi.org/10.21203/rs.3.rs-98526/v1

Abstract

Background. High levels of the leucine-rich repeats and immunoglobulin-like domains protein 1 (LRIG1) in tumor tissue are associated with a survival benefit in early-stage non–small cell lung cancer (NSCLC) due to presently unknown mechanisms.

Methods. A panel of NSCLC cell lines was transduced with LRIG1 expression vectors. Cell proliferation, chemosensitivity, radiosensitivity, clonogenicity, and migration were measured *in vitro*. Mice were implanted with mixed-cell populations, and the fraction of LRIG1-overexpressing cells was compared among metastatic sites, primary tumors, and injected cell populations.

Results. Clonogenicity was reduced in LRIG1-overexpressing cell lines. Minor or no changes were observed in the other analyzed functions. LRIG1 was neither enriched nor depleted in tumor cell populations at different metastatic sites.

Conclusion. LRIG1 reduced clonogenicity *in vitro*, but no other single underlying mechanism for LRIG1 tumor suppression in NSCLC was identified. Cell lines established from advanced NSCLC might not be a suitable model for mechanistic studies of early-stage disease.

Background

Lung cancer is the most common cause of cancer-related deaths worldwide (1, 2). Current lung cancer treatment is mainly based on clinical stage. For advanced disease, predictive biomarkers are used, but so far no prognostic or predictive markers are in routine clinical use for early-stage disease (3–6). Currently, postoperative adjuvant chemotherapy is recommended to patients based on stage only. New molecular markers to guide clinical decision making in early-stage disease are therefore needed. Leucine-rich repeats and immunoglobulin-like domains protein 1 (LRIG1) is a newly described prognostic marker in early-stage non–small cell lung cancer (NSCLC) (7). However, it is not known if and how LRIG1 influences the course of NSCLC or if LRIG1 expression is only a reflection of other important traits of the disease.

The LRIG family of proteins consists of three paralogs: LRIG1, LRIG2, and LRIG3. LRIG1 is the most well-characterized of the three family members, and it acts as an endogenous inhibitor of multiple receptor tyrosine kinases (RTKs). Inhibitory effects from LRIG1 have been observed on ErbBs 1–4 (including EGFR) (8, 9), RET (10), MET (11), PDGFRA (12), and AXL (13). The expression of LRIG1 in tumor tissue is associated with better survival in several human cancers, including carcinoma of the breast (14), uterine cervix (15, 16), bladder (17), prostate (18), melanoma (17), oligodendroglioma (17), cutaneous squamous cell carcinoma (19), and NSCLC. In NSCLC, high levels of LRIG1 in tumor tissue confer a large survival benefit in early-stage lung adenocarcinoma (7, 20), especially in tumors with low levels of the LRIG1-interacting protein LIM domain only protein 7 (LMO7) (21). The survival benefit of LRIG1 in NSCLC appears to be limited to early clinical stages, for which adjuvant chemotherapy is offered in order to prevent the development of metastatic disease. Therefore, it is reasonable to hypothesize that LRIG1 sensitizes cells to chemotherapy, which is in line with previous findings showing that ectopic LRIG1 expression confers increased sensitivity to cisplatin and vinorelbine in cells (22–25). Alternatively, LRIG1 might exert an inhibitory effect on the steps involved in the metastatic process. The metastatic process is incompletely characterized and involves multiple steps, from epithelial-to-mesenchymal transition, invasion into surrounding tissue and out into blood vessels, survival in circulation, extravasation, and establishment of a metastatic niche in a target organ (26–28). In this respect, in cancer cells *in vitro* LRIG1 has been shown to suppress both the epithelial-to-mesenchymal transition and invasion (11, 25, 29, 30).

In the present study, we analyzed possible effects of LRIG1 overexpression on hallmark features in NSCLC cells using *in vitro* assays of cell proliferation, chemosensitivity, radiosensitivity, clonogenicity, and migration and by developing an *in vivo* mouse model of hematogenous micrometastatic disease.

Methods

Expression vectors

The bicistronic lentiviral expression vectors pLVX-IRES-ZsGreen1 and pLVX-IRES-mCherry were obtained from Takara Bio (Kyoto, Japan) and used to assemble vectors pLVX-LRIG1-IRES-ZsGreen1 and pLVX-LRIG1-IRES-mCherry. A human full-length LRIG1 cDNA (Gene bank accession no. AF381545) was PCR amplified using CloneAmp HiFi premix (Takara Bio) with forward and reverse primers, both containing 15 bases that are complementary with the p3xFLAG-CMV-13 vector (Sigma-Aldrich, St. Louis, MO, USA) at their 5′ ends. All PCR primer and probe sequences are listed in supplemental Table 1. The p3xFLAG-CMV-13 vector was linearized using FastDigest HindIII and EcoRV restriction enzymes (Fermentas Sweden AB, Fisher Scientific, Gothenburg, Sweden) run on agarose gel, excised and eluted from the gel using an EZNA Gel Extraction Kit (Omega Bio-Tek, Norcross, GA, USA). The LRIG1 amplicon was cloned into the linearized p3xFLAG-CMV-13 vector in a seamless Golden Gate–type assembly, using an In-Fusion HD EcoDry kit (Takara Bio) as per the manufacturer's instructions, using a 2:1 molar ratio for the insert and vector, followed by transformation of NEB 5-alpha competent E. coli (Takara Bio) and plasmid preparation. From this plasmid, the FLAG-tagged full-length human *LRIG1* was PCR amplified using forward and reverse primers that contained 15 base sequences that were identical to the intended fusion sites in the final bicistronic recipient plasmids pLVX-IRES-ZsGreen1 and pLVX-IRES-mCherry. Using the same methods as above, the plasmids were linearized using NdeI and BamHI restriction enzymes (Fermentas Sweden AB), then purified and co-incubated with the *LRIG1*-containing amplicon in separate In-Fusion reactions. Sequencing primers were designed to cover the reference sequence of *LRIG1* and 200 bp 5′ and 3′ of the predicted insertion sites of both expression vectors (here referred to as pLVX-LRIG1-IRES-ZsGreen1 and pLVX-LRIG1-IRES-mCherry), and the purified vectors were sequenced to verify that the sequences and insertion sites were correct.

Cell culture and lentiviral transduction

The NSCLC cell lines H1975, H1299, HCC827, H520, and A549 were obtained from the American Type Culture Collection (ATCC, Manassas, VA, USA) and were cultured in RPMI 1640 medium supplemented with 10% fetal bovine serum (FBS) and 50 µg/ml gentamicin. $H1975^{DoxLRIG1}$, $HCC827^{DoxLRIG1}$, $H520^{DoxLRIG1}$, and

A549^{DoxLRIG1} cells with doxycycline-inducible LRIG1 expression were generated by transducing the parental cell lines with pLVX-LRIG1-TRE3G and pLVX-Tet3G, as previously described (31).

Lentiviral particles carrying pLVX-LRIG1-IRES-ZsGreen1, pLVX-IRES-ZsGreen1, pLVX-LRIG1-IRES-mCherry, and pLVX-IRES-mCherry were generated by transfecting Lenti-X cells (Takara Bio) with the vectors as per the manufacturer's instructions. H1299 and H1975 cells were stably transduced with all four of the above-mentioned lentiviral particles by incubation with 700 µl of fresh culture medium, 1 µl of 6 mg/ml polybrene solution, and 300 µl of viral supernatant in 12-well culture plates, followed by centrifugation at 800x g for 1 hour at room temperature. To control for artifacts due to clonal variation, all transductions were carried out in duplicates and kept separate from each other, resulting in two separate cell line variants for each combination of cell line and viral vector. Transduced cells were isolated by two sequential fluorescence-activated cell sortings on a FACSAria cell sorter (BD Biosciences, East Rutherford, NJ, USA) using a 488 nm laser with a 510/21 filter (for ZsGreen1) or a 550 nm laser with a 585/42 filter (for mCherry). The 16 resulting cell line variants were verified to be pathogen-free at IDEXX BioAnalytics (Ludwigsburg, Germany). The H1975^{DoxLRIG1}, HCC827^{DoxLRIG1}, H520^{DoxLRIG1}, and A549^{DoxLRIG1} cell lines as well as one of the H1975-LRIG1-IRES-mCherry cell lines and one of the H1299-LRIG1-IRES-mCherry cell lines were authenticated with regard to their original parental cell lines through short tandem repeat profiling via IDEXX BioAnalytics.

Western blotting

Cells were cultured to 90% confluency in 30 mm wells and then lysed using 250 µl of cell extraction buffer (Thermo Fisher, Waltham, MA, USA) with added Complete EDTA-free protease inhibitor cocktail (Roche, Basel, Switzerland) for 30 minutes at 4 °C, then centrifuged at 20,000x g for 10 minutes. Protein concentrations in the cleared lysates were determined using a Pierce BCA assay kit (Thermo Fisher) by measuring linear absorbance at 562 nm on a NanoDrop spectrophotometer (Thermo Fisher) and comparing to a pre-diluted albumin standard as per the manufacturer's instructions. Prior to analysis, lysates were diluted in lysis buffer to the same protein concentrations, then denatured through the addition of LDS buffer and reducing agent (Thermo Fisher), followed by incubation at 70 °C for 10 minutes. The proteins were separated via gel electrophoresis using a 3–8% Tris-Acetate PAGE gel (Thermo Fisher), followed by semi-dry transfer to an LF PVDF membrane (Bio-Rad, Berkeley, CA, USA) using a TurboTransfer machine (Bio-Rad). Membranes were blocked using Odyssey PBS blocking buffer (Li-Cor, Lincoln, NE, USA). The primary antibodies used, and their dilutions, were mouse anti-actin, 1:7,500 (Abcam, Cambridge, UK), and rabbit anti-LRIG1, 1:1,000 (AgriSera, Vännäs, Sweden). The secondary antibodies used, and their dilutions, were goat anti-rabbit IgG IRDye 680 and goat anti-mouse IRDye 800 (Li-Cor), both at 1:15,000. Membranes were incubated with the respective antibodies for 1 hour at room temperature and washed using TBST (20 mM Tris, 150 mM NaCl and 0.1% Tween 20) in a Freedom Rocker BlotBot (Next Advance, Troy, NY, USA), then scanned at 700 and 900 nm using an Odyssey imager (Li-Cor) at 84 µm resolution.

Live-cell proliferation and migration assays

For all live-cell assays, cells were seeded at a density of 10,000 cells per cm² in either standard 6-well or Sarstedt Lumox 24-well plates. To induce LRIG1 expression in LRIG1-inducible cells, 1 µg/ml of doxycycline was added. Plates were incubated overnight. Prior to recording, wells were washed once in PBS to remove debris, resupplemented with standard cell culture medium, covered with HoloLids (Phase Holographic, Lund, Sweden), and inserted in a HoloMonitor holographic microscope (Phase Holographic) mounted inside a standard cell culture incubator. Live-cell imaging was performed on 16 predefined 0.52 × 0.52 mm areas per well, which were continuously recorded at 8-minute intervals for 48 hours. Proliferation curves were created by measuring the cell count in each area at 1-hour intervals, and doubling time was calculated by comparing cell counts at $t = 0$ and $t = 48$ hours. Cell migration, measured as average cell motility in µm/hour, was calculated by tracking individual cell movements on a frame by frame basis.

Competitive cell proliferation assay

For competitive cell proliferation, H1299$^{LRIG1\ -\ ZsGreen1}$ cells were pooled together with H1299$^{control\ -\ mCherry}$ and H1299$^{LRIG1\ -\ mCherry}$ cells with H1299$^{control\ -\ ZsGreen1}$, both in a 1:1 fashion, using three separately transduced clones of each vector. Tubes containing cell suspensions were subsequently labeled in a blinded fashion, and cells were plated onto 6-well tissue culture plates (Sarstedt AG, Nümbrecht, Germany) supplied with a standard medium containing 10% FBS. The plates were incubated for up to 18 days, with replacement of the growth medium when needed. Cells were lysed at 0, 3, 8, 11, 15, and 18 days using a DNEasy blood and tissue kit (Qiagen, Venlo, Netherlands), and the ratio of *LRIG1* to control vector gene copies was determined using digital droplet PCR (ddPCR) as described in the section below.

Chemosensitivity assay

To analyze chemosensitivity, four separately transduced LRIG1 over-expressing H1299 or H1975 cell lines and four separately transduced vector control H1299 or H1975 cell lines were plated in triplicates onto 96-well plates with 4,000 cells per well and incubated overnight. A cell culture medium was prepared with added cisplatin (Sigma-Aldrich) in concentrations ranging from 10 to 100 µmol/l, and with vinorelbine tartrate (Sigma-Aldrich) in concentrations ranging from 60 to 1,560 nmol/l, then added to the triplicate wells 24 hours after plating. Fresh medium was added to the control wells. Cell viability was measured 1 hour after plating, at the start of treatment, and at 24, 60, and 72 hours after treatment start. Viability was measured using the resazurin reduction assay, as previously described (32), replacing the medium in each well with 10 µl 0.4 mg/ml resazurin solution and 90 µl culture medium, then incubating at 37 °C for 4 hours and measuring fluorescence using a SpectraMax i3x spectrophotometer (Molecular Devices, San Jose, CA, USA) set to excitation = 530 nm and emission = 590 nm. IC_{50} was determined through logarithmic regression. For each drug concentration, a time-independent growth rate, GR(c), as described by Hafner et al. (33), was calculated by normalizing the viability of paired untreated controls at each time point.

Clonogenic assay

To analyze clonogenicity, cells were detached using trypsin, resuspended in culture medium, then counted, diluted, and plated onto 6-well tissue culture plates at a density of 100 cells/cm². Stably transduced cells were plated in triplicates. LRIG1-inducible cells were plated onto all six wells, with 1 µg/ml doxycycline added to three wells. Once macroscopically visible colonies had formed, cells were fixated in methanol at − 20 °C for 10 minutes and then stained using 0.5%

crystal violet solution. Plates were dried and scanned in a GelDoc imager (Bio-Rad) in transillumination mode. Colonies were automatically counted in a blinded fashion using an ImageJ (34) macro [Additional file 1].

Radiosensitivity assay

To analyze radiosensitivity, cells were plated in 6-well tissue culture plates and grown to approximately 75% confluency. The plates were then irradiated to an absorbed dose of 1, 2, 4, 6, 8, or 10 Gy using a Clinac iX photon beam linear accelerator (Varian, Palo Alto, CA, USA). In order to avoid beam dispersion due to air gaps, each cell culture well was filled to the brim with culture medium and encased in rigid Perspex bolus blocks during treatment. Clonogenic assays were performed immediately after the radiation treatment. A clonogenic assay was performed on the treated cells using the same method as above, but with 300 cells per cm^2 seeded in triplicates for each radiation dose.

Transwell and wound closure assays

For the transwell migration assay, cells were plated and serum-starved in 0.1% FBS for 24 hours. PET membrane tissue culture inserts with a 4 µm pore size (Sarstedt AG) were placed on a 24-well plate. The cell culture wells were filled with medium with 10% FBS, while the inserts were filled with serum-free medium along with 5,000 cells. Each of the four cell line variants was plated in triplicates. Plates with inserts were put in a cell culture incubator for 12 hours, after which the inside of each membrane was swabbed and washed to remove stationary cells. Membranes with adherent migrated cells were subsequently fixated with methanol for 10 minutes at − 20 °C and stained using Meyer's hematoxylin and labeled in a blinded fashion. Cells were counted manually.

For the wound closure assay, the cells were plated into 6-well tissue culture plates and grown to a 75% confluent monolayer, after which a cross-shaped wound was made by scraping a plastic pipette tip across the surface. Wells were washed twice in PBS to remove detached cells. Fresh medium with 10% FBS was added, and the plates were kept in a cell culture incubator. At predefined time intervals, the wound was imaged using a Zeiss AxioCam ICC1 and an Axio A1 phase contrast microscope (Carl Zeiss AG, Oberkochen, Germany) with a 10x lens. The wound area was quantified in an automated blinded fashion using an ImageJ script (34) [Additional file 2]. Wound closure rates were calculated for each well using linear regression, and a ratio was calculated by dividing the closure rate of LRIG1 over-expressing cells with the closure rate of the vector controls.

Mouse strains and animal husbandry

Female CIEA NOG mice (Taconic, Ejby, Denmark) were kept in individually filtered ventilated racks in a controlled environment with a constant 27 °C temperature and a 12-hour light cycle. Mice were fed standard chow and watched daily for symptoms. All animal experiments were performed according to the Swedish animal welfare law and with ethical approval from the regional animal welfare board (DNR A 28–15).

Orthotopic implantation and tissue analysis

For an initial investigation of the metastatic potential of a series of NSCLC cell lines, A549, H1299, H1975, and HCC827 cells were trypsinized and counted, then pelleted and resuspended on ice in RPMI 1640 medium with 20% added soluble matrix (Geltrex, Thermo Fisher) to a concentration of 2 × 10^6 cells/ml (A549 and H1299) or 1 × 10^7 cells/ml (H1975 and HCC827), of which individual aliquots of 50 µl (1 × 10^5 cells or 5 × 10^5 cells, respectively) were prepared for each animal. Cell suspensions were kept on ice until implantation to avoid matrix solidification. Animals were anesthetized using 5% isoflurane (Baxter, Deerfield, IL) in pure oxygen, and an ultrasound probe (Fujifilm VisualSonics, Toronto, ON, Canada) was used to identify the dorsal intercostal spaces. Cell suspensions were gently vortexed and stereotaxically injected into the left lung using a 16G needle through the sixth left intercostal space to a depth of 2 mm, with ultrasonographic confirmation that the injected suspension was inside the parenchyma. After 4 weeks, animals were anesthetized using 5% isoflurane, and a Bruker Bio-Spec 94/20 USR small animal MRI was used to obtain respiration-gated T1 FLASH sequences with the following parameters: TR = 113 ms, TE = 2.8 ms, flip angle = 30 degrees, field of view = 30 mm, matrix = 256 × 256 and 16 averages. Fifteen axial slices were obtained with 0.50 mm slice thickness and 1.00 mm interslice distance. A 40 mm quadrupolar volume coil was used in transmit/receive mode. Mice were euthanized immediately after imaging. For each animal, the left and right lung, brain, liver, and any other visceral organ with macroscopically visible metastases were fixated in 4% paraformaldehyde, paraffin-embedded, sectioned, and H&E stained.

For the second experiment, pooled cell suspensions were prepared in triplicates in a 1:1 fashion, with separate H1299 LRIG1-ZsGreen clones pooled with H1299 control-mCherry cells, and inversely, with H1299 LRIG1-mCherry cells pooled with H1299 control-ZsGreen cells. Cell suspensions were then injected as a primary tumor in the left lung using the method described above, in a double-blinded fashion, with 0.5 × 10^6 cells per animal. A 500 µl sample of each injected cell suspension was kept at − 20 °C in order to compare the composition of the tumors with that of the injected cells. Animals were euthanized at the first sign of symptoms, or after 4 weeks if they did not develop symptoms. For each animal, the left lung was longitudinally cut through the middle of the primary tumor, and the four lobes of the right lung were separated. Representative samples were taken from the liver and mediastinal lymph nodes if macroscopic metastases were visible. Genomic DNA was isolated from the stored cell suspensions, half of the left lung, two of the right lobes (middle and postcaval), and representative samples of macrometastases, using a DNEasy blood and tissue kit (Qiagen). The other half of the left lung, the superior lobe of the right lung, and representative samples of micrometastases were fixated in 95% ethanol and paraffin-embedded.

Digital droplet PCR

To quantify the numbers of integrated *ZsGreen1* and *mCherry* gene copies or *Lrig3*, used as a mouse genomic reference, ddPCR was used. The primer and probe sequences used are summarized in supplemental Table 1. Genomic DNA samples were restriction digested using KpnI with added 10x FastDigest buffer (Fermentas Sweden AB) at 37 °C for 60 minutes, followed by heat inactivation at 80 °C for 3 minutes. PCR reactions were prepared using 900 nM of forward and reverse primers for gene 1 (*mCherry* or *ZsGreen1*) and gene 2 (*ZsGreen1* or *Lrig3*), 250 nM of FAM probe for gene 1, 250 nM of HEX probe for gene 2, 10 µl ddPCR supermix without dUTP (Bio-Rad), 240 ng of sample DNA, and nuclease-free water, up to a total volume of 20 µl. Droplets were generated by adding 20 µl of PCR reaction and 70 µl droplet-generation oil into the corresponding wells in a droplet-generation cartridge (Bio-Rad), which was then processed in a QX1000 droplet generator (Bio-Rad) and transferred onto a PCR plate. Each plate was run for 10 min at 95 °C, followed by 40 cycles of 95 °C for 30 sec and

56 °C for 60 sec, then a final step at 98 °C for 10 min, then analyzed in a ddPCR droplet analyzer (Bio-Rad), with automatic identification of positive droplets in the FAM and HEX channels if possible, or else using manual thresholding at a signal amplitude of 1500. For each sample, a ratio was calculated by dividing the number of positive droplets corresponding to the *LRIG1* overexpressing vector (in either the FAM or HEX channel) by the number of positive droplets corresponding to the control vector. For the animal tissue DNA samples from the left lung containing a primary tumor, the obtained ratio was normalized against the corresponding ratio in the injected cell suspension. For samples corresponding to metastatic sites, the LRIG1-to-vector control ratio was normalized against the primary tumor.

Data analysis and statistics

Statistical significance of paired populations at single time points, drug concentrations, or radiation doses was analyzed using the independent samples *t*-test. Comparisons against fixed values were done using the one-sample *t*-test. Comparisons between multiple populations or analysis of multiple repeated measurements were performed using the Wilcoxon signed-rank sum test. IC50 values were determined using logistic regression. For comparisons of data not normally distributed, the Mann-Whitney *U* test was used. All statistical analyses were performed in Jamovi (35, 36). A p-value of < 0.05 was considered significant.

Results

LRIG1 overexpression did not affect cell proliferation in most NSCLC cell lines in vitro

To investigate whether LRIG1 affects the proliferation rates of NSCLC cells, LRIG1 was ectopically overexpressed in a series of NSCLC cell lines, followed by analyses of the proliferation rates of the wild-type and LRIG1-overexpressing cells. At no time point did the proliferation rates of the LRIG1 overexpressing $H1299^{LRIG1\ -\ mCherry}$ and $H1975^{LRIG1\ -\ mCherry}$ cell lines differ significantly from their vector control counterparts, $H1299^{control\ -\ mCherry}$ and $H1975^{control\ -\ mCherry}$, respectively (Fig. 1A, Student's *t*-test, $p = 0.373$ and $p = 0.056$, respectively). Also, no significant differences could be observed between the cell populations based on fluorescent reporter ($p = 0.227$ for H1299 and $p = 0.547$ for H1975; data not shown), indicating that the fluorescent reporters themselves had no effect on the cell proliferation rates. In our additional panel of LRIG1-inducible NSCLC cells, the only significant difference in proliferation rate was observed for HCC827, in which LRIG1 overexpression was associated with a reduced proliferation rate (i.e., an increased population doubling time) ($p = 0.042$). Again, a non-significant trend towards a slower proliferation rate for LRIG1-overexpressing H1975 cells was observed ($p = 0.057$). The proliferation rates in A549 and H520 were unaffected by the induction of LRIG1 expression ($p = 0.875$ and $p = 0.267$, respectively).

In a competitive proliferation assay, no statistically significant changes were observed in the relative proportion of LRIG1 overexpressing cells when co-cultured with control cells and grown past confluency in a dense monolayer. At 18 days, the relative proportion of LRIG1-overexpressing cells had seemingly decreased, but not significantly so (Fig. 1B, Student's *t*-test, $p = 0.352$).

Taken together, the cell proliferation experiments showed that changes in proliferation rate in LRIG1-overexpressing cells were only minor, and overexpressing cells were not outcompeted by vector controls in a mixed-cell population.

NSCLC chemosensitivity was unaffected by LRIG1 overexpression in vitro

To see if ectopic overexpression of LRIG1 affected the chemosensitivity in NSCLC cell lines, cytotoxic assays were performed on H1299 and H1975 cells treated with cisplatin or vinorelbine. Cisplatin-induced cytostasis and cell death occurred at similar concentrations for H1299 and H1975, with no significant differences between vector controls and LRIG1 overexpressing cells. For H1299, mean IC_{50} was 34.9 µmol/l for vector controls and 35.8 µmol/l for LRIG1-overexpressing cells. The difference was not significant (Fig. 2A, Mann-Whitney *U* test, $p = 0.984$). Mean IC_{50} for H1975 vector controls was 24.0 µmol/l, compared to 34.1 for LRIG1-overexpressing cells, but the difference was not significant ($p = 0.060$).

Vinorelbine potently induced cytostasis for both H1299 and H1975 cells at extremely low concentrations but failed to induce cytotoxicity, as cells remained alive but non-replicating, even at high drug concentrations; therefore, IC_{50} could not be reliably determined. When comparing vector controls with LRIG1-overexpressing cells, no significant curve separation was seen for H1299 (Fig. 2B, Wilcoxon rank-sum test, $p = 0.298$) or H1975 ($p = 0.152$).

Thus, no changes in cisplatin or vinorelbine chemosensitivity were observed when LRIG1 was overexpressed in H1299 and H1975 cells.

LRIG1 overexpression did not affect radiosensitivity but affected clonogenicity

To determine whether ectopic LRIG1 overexpression affected the radiosensitivity of H1299 and H1975 cells, a clonogenic assay was performed. H1299 vector control cells had significantly reduced clonogenicity after treatment with radiation doses of 4 Gy or higher (paired samples *t*-test, $p = 0.041$, Fig. 2C), whereas H1975 cells had significantly reduced clonogenicity from 2 Gy onwards ($p = 0.003$, Fig. 2D). For both H1299 and H1975, LRIG1-overexpressing cells did not exhibit any significant differences in clonogenicity compared to vector control cells at any radiation dose, indicating that LRIG1 overexpression did not significantly affect the radiosensitivity in these cells.

A separate experiment was performed to measure the effects of LRIG1 overexpression on the baseline colony-forming ability of more sparsely plated non-irradiated NSCLC cells. This experiment showed a general decrease in clonocenicity in LRIG1-overexpressing cells (Fig. 2E). Significant decreases in the number of colonies were observed for LRIG1-overexpressing H1299 (Student's *t*-test, $p < 0.001$), H1975 ($p = 0.033$), and HCC827 ($p = 0.041$), but not for A549 ($p = 0.872$) or H520 ($p = 0.467$).

Cell migration was mostly unaffected by LRIG1 overexpression

To investigate the effects of ectopic LRIG1 overexpression on cell migration, we performed long-term holographic live-cell imaging, as well as wound closure assays and standard transwell migration assays, using a panel of NSCLC cell lines. Under unstimulated conditions, with live-imaged cells, a significant increase in motility rate was observed for LRIG1-overexpressing H1299, A549^{TetLRIG1}, H520^{TetLRIG1}, and HCC827^{TetLRIG1} cells, while a significant decrease in motility rate was observed for LRIG1-overexpressing H1975^{TetLRIG1} cells. However, the differences in motility were, in general, only minor (Fig. 3A).

In the wound closure assay, LRIG1-overexpressing H1299 cells closed the wound area slightly faster than control cells, a difference that was nevertheless significant overall and with significant differences at all time points (Fig. 3B and C). When calculating the relative wound closure rate, the LRIG1-overexpressing cells bridged the area at a rate of 4.16% per hour, compared to 3.57% per hour for control cells (Mann-Whitney *U* test, $p = 0.029$) For H1975, the LRIG1-overexpressing cells bridged the gap at a rate similar to that of the control cells, with a relative closure rate 2.28% vs. 2.21% per hour (Mann-Whitney *U* test, $p = 0.857$).

In the transwell migration experiments, no statistically significant difference in migrated cells could be observed between LRIG1-overexpressing H1299 cells or H1975 cells compared to their respective vector control cells (Student's *t*-test, $p = 0.264$ and $p = 0.356$, respectively) (Fig. 3D). No significant differences in cell migration were observed when evaluating the effect of fluorescent reporters on either cell line ($p = 0.109$ and 0.694, respectively).

Taken together, LRIG1 overexpression affected the cell motility of all cell lines except one of the H1975 cell lines. However, the effects of LRIG1 on cell motility and migration were not consistent—both positive and negative—and were generally small.

Orthotopically implanted H1299 cells gave rise to hematogenous micrometastases

To be able to assess the influence of LRIG1 on NSCLC metastases *in vivo*, we first screened four cell lines (A549, H1975, HCC827, and H1299) for metastatic potential when implanted orthotopically in immunodeficient mice (Supplemental Table 2). Mice injected with A549 cells remained asymptomatic, and no tumor cells could be observed in tissue sections of either the implantation site of the left lung or in any other organ. For HCC827, mice remained asymptomatic, with normal behavior throughout the observation period; however, extensive tumor growth was observed at the implantation site. No metastases were observed in any other parenchymal organ. Mice injected with H1975 became symptomatic starting at week 3 of observation, with tachypnoea and visible cyanosis in the tail. MRI sequences showed extensive bilateral pleural effusion and pathologically enlarged mediastinal lymph nodes. Histopathologic evaluation showed tumor growth at the implantation site and bilateral nodes on the visceral pleura. One mouse had a macroscopically visible metastasis in the tail of the pancreas. For mice injected with H1299, symptomatology and development over time were identical to the H1975 mice, and the MRI evaluation also showed pleural effusion, as well as enlarged mediastinal lymph nodes (Fig. 4A). Injection sites showed tumor growth, and both lungs on most animals exhibited hematogenous micrometastases in the form of numerous spindle-shaped cell clusters embedded in the alveolar walls, deep in the lung parenchyma (Fig. 4B). Additionally, one mouse had a macroscopically visible subcutaneous metastasis on the thoracic wall, contralateral to the injection site.

LRIG1-overexpressing H1299 cells had a competitive advantage when orthotopically implanted

Finally, we sought to investigate whether LRIG1 overexpression conferred a selective disadvantage or advantage on H1299 cells at the primary tumor implantation site or in the metastatic process *in vivo*. This was assessed by injecting a pooled population of H1299 cells, with a 1:1 ratio between LRIG1-overexpressing cells and vector control cells, orthotopically into the left lung of immunocompromised mice and then comparing the ratio between LRIG1 vectors and control vectors in tumor DNA prepared from the injected cell populations, primary tumors, and metastatic sites. After implantation, 21 of 24 injected mice became symptomatic starting at week 3 of observation. Symptoms were the same as the initial experiment, except for one mouse that presented with flaccid paresis of the hind legs, later found to be due to spinal cord overgrowth from the primary tumor at the mid-thoracic level. In total, 18 left lungs with macroscopically visible primary tumors, 18 right lungs with detectable micrometastases, 5 livers with macroscopically visible metastases, and 3 intact mediastinal lymph node metastases were included in our analysis.

When comparing the ratio of *LRIG1* to control vector, we found an enrichment of *LRIG1* in primary tumors compared to the ratio in the injected cell suspension, indicating that the cell population with *LRIG1* overexpression had a competitive advantage over the control population in establishing a primary tumor after injection. Regarding our primary outcome, the composition of hematogenous micrometastases in the right lung, no significant trends could be observed when comparing the LRIG1-to-control vector ratio between the micrometastases and their corresponding primary tumors (Fig. 4C).

Discussion

In this study we investigated possible mechanisms that could account for the observed association between high LRIG1 expression and increased survival among early-stage NSCLC patients. To this end, we overexpressed LRIG1 in a series of NSCLC cell lines and monitored possible effects on cell proliferation, sensitivity to chemotherapy and radiotherapy, and colony formation and migration, as well as the cellular competitiveness in an *in vivo* model of NSCLC metastasis. Table 1 provides an overview of the results for all cell lines. Overall, the only consistent effect of LRIG1 that we could detect was reduced colony-formation efficiency among the LRIG1-overexpressing cells. This could imply that LRIG1-expressing circulating tumor cells have a decreased ability to form viable metastases (colonies) in the metastatic niche, which clearly warrants further investigation.

Table 1
Summary of the observed effects of LRIG1 overexpression in NSCLC cell lines.

Cell line	LRIG1 overexpression level	Proliferation rate	Motility	Wound healing	Transwell assay	Clonogenicity	Cisplatin sensitivity	Vinorelbine sensitivity	Radiosensivity	Primary tumor vs. injected population
H1975	High *	ns	ns	ns	ns	↓ *	ns	ns	ns	
H1299	High *	ns	↑ ***	↑ **	ns	↓ ***	ns	ns	ns	↑*
A549 TetOn	Low *	ns	—			ns				
H1975 TetOn	High **	ns	—			↓ *				
H520 TetOn	ns	ns	—			ns				
HCC827 TetOn	High ***	↓ *	—			↓ *				

A previous report suggested that overexpression of LRIG1 in the EGFR-mutated HCC827 cell line strongly suppressed cell proliferation, invasion, and migration *in vitro* and consequently also inhibited subcutaneous tumor growth *in vivo* (30). Our results confirmed the anti-proliferative effect of LRIG1 on this cell line; however, we did not observe a suppressed migration. Instead, the induced expression of LRIG1 resulted in increased motility in our HCC827 cells. The reason for this discrepancy between our results and the previous study is not known. Nevertheless, the confirmed suppression of HCC827 cell proliferation may suggest an important role for LRIG1 in EGFR-mutated NSCLC. The latter would be in agreement with the originally proposed mechanism of action for LRIG1 as an endogenous EGFR inhibitor (8) and is also in line with the general findings and conclusions of Torigoe et al. (30). Notably, however, we did not observe a general suppression of cell proliferation in response to LRIG1 overexpression among the analyzed NSCLC cell lines, which could suggest that its effects on cell proliferation might only partly explain the survival benefit associated with LRIG1 expression in NSCLC.

In contrast to other reports, we did not consistently observe reduced migration rates or increased sensitivity to chemotherapy or radiotherapy among LRIG1-overexpressing cells. Regarding cell motility and migration, our results were contradictory. Four LRIG1-overexpressing cell lines showed increased motility, and one showed decreased motility. The LRIG1-overexpressing H1299 and H1975 cell lines showed an increased migration rate in the wound healing assay, while they showed a decreased migration rate in the transwell assay. Previous studies have shown that LRIG1 decreases *in vitro* migration in melanoma and glioma cell lines through pathways downstream of EGFR (37, 38). However, that does not seem to be a consistent finding among the NSCLC cell lines tested in this study. Similarly, in contrast to previous studies in other cancer cell types, our LRIG1-overexpressing NSCLC cell lines did not show increased sensitivity to cisplatin, vinorelbine, or radiation. An LRIG1-mediated increase in radiosensitivity, attributed to down-regulation of EGFR signaling, has previously been described for U-251 glioma cells (39). Despite the fact that one of the NSCLC cell lines in our study harbored an EGFR driver mutation (HCC827), this cell line's radiosensitivity remained unaffected by LRIG1 overexpression as well. One possible clinical implication of our *in vitro* treatment results is that LRIG1 expression may not be a candidate predictive marker for chemotherapy or radiotherapy in NSCLC.

Regrettably, only one of our tested NSCLC cell lines, H1299, formed hematogenous micrometastases in mice. Therefore, we were restricted to H1299 for our experiments to directly address the role of LRIG1 in the metastatic spread of orthotopically implanted NSCLC. *In vitro*, LRIG1-overexpressing H1299 cells showed, on one hand, increased motility and migration rates, and on the other hand, decreased colony-formation capacity. Nevertheless, *in vivo*, overexpression of LRIG1 in H1299 cells appeared to confer a competitive advantage during establishment of the primary tumor but did not affect the metastatic potential of the cells. These results are interesting but do not explain increased survival among patients with high LRIG1 expression. Despite the inconclusive results of the mouse experiments, the *in vivo* model might be useful for studies of other mechanisms in NSCLC metastasis. As far as we know, this is the first time ddPCR on whole organ lysates has been used to quantify differences in cell populations between primary tumors and micrometastatic sites. Orthotopic implantation is an efficient model of hematogenous metastasis that often gives rise to a high metastatic burden (40), and our model provides an unbiased way of detecting and quantifying micrometastases with high throughput.

Notably, whereas the previously observed survival benefit of high LRIG1 expression is limited to early-stage NSCLC cases, all of the cell lines used in the present study were established from individuals harboring stage III or IV disease. Thus, the cell lines used may not be representative of the NSCLC types where LRIG1 has the strongest impact. Regrettably, there is a shortage of available NSCLC cell lines that are established from early-stage disease. Therefore, it would be desirable to establish new cell lines from early-stage disease by using tumor tissue from percutaneous transthoracic biopsies in order to more accurately study the mechanisms of early-stage disease.

Conclusions

In summary, although our results did not reveal a clear mechanistic link between high LRIG1 expression and favorable survival in early-stage NSCLC, the observed association between high LRIG1 expression and poor NSCLC cell clonogenicity may be worth exploring further. It may also be desirable to establish improved experimental models that better recapitulate the key features of early-stage NSCLC.

Abbreviations

ddPCR Digital droplet PCR

FBS Fetal bovine serum

GR(c) Concentration-dependent growth rate

IC50 50% inhibitory growth concentration

MRI Magnetic resonance imaging

NSCLC Non–small cell lung cancer

PBS Phosphate buffered saline

RTK Receptor tyrosine kinase

TBST Tris-buffered saline with Tween 20 detergent

Declarations

Acknowledgments

We thank Magnus Karlsson for performing cell irradiation.

Funding

This investigation was supported by grants from the Cancer Research Foundation in Northern Sweden, the Swedish Cancer Society, and the Västerbotten Regional Council.

Availability of data and materials

All the experimental data analyzed and displayed in the present manuscript are available from the corresponding author upon reasonable request.

Affiliations

Department of Radiation Sciences, Medical faculty, Umeå University, S-901 87 Umeå, Sweden
Samuel Kvarnbrink, Håkan Hedman, Mikael Johansson

Contributions

SK performed the experiments with technical guidance from HH, performed data collection and analysis, contributed to the design of the study and wrote the manuscript. MJ and HH conceived the idea, designed the study, co-wrote and edited the manuscript. All authors have read and approved the manuscript.

Corresponding author

Correspondence to Samuel Kvarnbrink, samuel.kvarnbrink@umu.se

Ethics approval

All animal experiments were performed according to the Swedish animal welfare law and with ethical approval from the regional animal welfare board (DNR A 28–15).

Consent for publication

Not applicable.

Competing interests

The authors have no competing interests to declare.

References

1. Ferlay J, Steliarova-Foucher E, Lortet-Tieulent J, Rosso S, Coebergh JWW, Comber H, et al. Cancer incidence and mortality patterns in Europe: estimates for 40 countries in 2012. Eur J Cancer. 2013 Apr;49(6):1374–403.
2. Fitzmaurice C, Abate D, Abbasi N, Abbastabar H, Abd-Allah F, Abdel-Rahman O, et al. Global, Regional, and National Cancer Incidence, Mortality, Years of Life Lost, Years Lived With Disability, and Disability-Adjusted Life-Years for 29 Cancer Groups, 1990 to 2017: A Systematic Analysis for the Global Burden of Disease Study. JAMA Oncol. 2019 Sep 27;5(12):1749–68.
3. Kelly K, Altorki NK, Eberhardt WEE, O'Brien MER, Spigel DR, Crinò L, et al. Adjuvant Erlotinib Versus Placebo in Patients With Stage IB-IIIA Non-Small-Cell Lung Cancer (RADIANT): A Randomized, Double-Blind, Phase III Trial. J Clin Oncol. 2015 Dec 1;33(34):4007–14.
4. Goss GD, O'Callaghan C, Lorimer I, Tsao M-S, Masters GA, Jett J, et al. Gefitinib Versus Placebo in Completely Resected Non–Small-Cell Lung Cancer: Results of the NCIC CTG BR19 Study. JCO. 2013 Sep 20;31(27):3320–6.
5. Wakelee HA, Dahlberg SE, Keller SM, Tester WJ, Gandara DR, Graziano SL, et al. Adjuvant chemotherapy with or without bevacizumab in patients with resected non-small-cell lung cancer (E1505): an open-label, multicentre, randomised, phase 3 trial. Lancet Oncol. 2017 Dec;18(12):1610–23.
6. Herbst RS, Tsuboi M, John T, Grohé C, Majem M, Goldman JW, et al. Osimertinib as adjuvant therapy in patients (pts) with stage IB–IIIA EGFR mutation positive (EGFRm) NSCLC after complete tumor resection: ADAURA. JCO. American Society of Clinical Oncology; 2020 Jun 20;38(18_suppl):LBA5–LBA5.
7. Kvarnbrink S, Karlsson T, Edlund K, Botling J, Lindquist D, Jirström K, et al. LRIG1 is a prognostic biomarker in non-small cell lung cancer. Acta Oncol. 2015;54(8):1113–9.
8. Gur G, Rubin C, Katz M, Amit I, Citri A, Nilsson J, et al. LRIG1 restricts growth factor signaling by enhancing receptor ubiquitylation and degradation. EMBO J. 2004 Jul 29;23(16):3270–81.
9. Laederich MB. The Leucine-rich Repeat Protein LRIG1 Is a Negative Regulator of ErbB Family Receptor Tyrosine Kinases. J Biol Chem. 2004 Aug 16;279(45):47050–6.
10. Ledda F, Bieraugel O, Fard SS, Vilar M, Paratcha G. Lrig1 Is an Endogenous Inhibitor of Ret Receptor Tyrosine Kinase Activation, Downstream Signaling, and Biological Responses to GDNF. J Neurosci. 2008 Jan 2;28(1):39–49.
11. Shattuck DL, Miller JK, Laederich M, Funes M, Petersen H, Carraway KL, et al. LRIG1 Is a Novel Negative Regulator of the Met Receptor and Opposes Met and Her2 Synergy. Mol Cell Biol. 2007 Feb 13;27(5):1934–46.
12. Rondahl V, Holmlund C, Karlsson T, Wang B, Faraz M, Henriksson R, et al. Lrig2-Deficient Mice Are Protected against PDGFB-Induced Glioma. Kotliarova S, editor. PLoS ONE. 2013 Sep 4;8(9):e73635–18.
13. Neirinckx V, Hau A-C, Schuster A, Fritah S, Tiemann K, Klein E, et al. The soluble form of pan-RTK inhibitor and tumor suppressor LRIG1 mediates downregulation of AXL through direct protein–protein interaction in glioblastoma. Neuro-Oncol Adv. 2019 Sep 6;1(1):1117–12.
14. Krig SR, Frietze S, Simion C, Miller JK, Fry WHD, Rafidi H, et al. Lrig1 is an estrogen-regulated growth suppressor and correlates with longer relapse-free survival in ERα-positive breast cancer. Mol Cancer Res. 2011 Oct 16;9(10):1406–17.
15. Lindström AK, Ekman K, Stendahl U, Tot T, Henriksson R, Hedman H, et al. LRIG1 and squamous epithelial uterine cervical cancer: correlation to prognosis, other tumor markers, sex steroid hormones, and smoking. Int J Gynecol Cancer. 2008 Mar;18(2):312–7.
16. Hedman H, Lindström AK, Tot T, Stendahl U, Henriksson R, Hellberg D. LRIG2 in contrast to LRIG1 predicts poor survival in early-stage squamous cell carcinoma of the uterine cervix. Acta Oncol. 2010 Aug;49(6):812–5.
17. Rouam S, Moreau T, Broët P. Identifying common prognostic factors in genomic cancer studies: A novel index for censored outcomes. BMC bioinformatics. BioMed Central; 2010 Dec 1;11(1):150.
18. Thomasson M, Wang B, Hammarsten P, Dahlman A, Persson JL, Josefsson A, et al. LRIG1 and the liar paradox in prostate cancer: A study of the expression and clinical significance of LRIG1 in prostate cancer. Int J Cancer. 2011 Apr 8;128(12):2843–52.
19. Tanemura A, Nagasawa T, Inui S, Itami S. LRIG-1 provides a novel prognostic predictor in squamous cell carcinoma of the skin: immunohistochemical analysis for 38 cases. Dermatol Surg. 2005 Apr;31(4):423–30.
20. An Y, Zhao Z, Ou P, Wang G. Expression of LRIG1 is Associated With Good Prognosis for Human Non-small Cell Lung Cancer. Medicine (Baltimore). 2015 Nov;94(47):e2081.
21. Karlsson T, Kvarnbrink S, Holmlund C, Botling J, Micke P, Henriksson R, et al. LMO7 and LIMCH1 interact with LRIG proteins in lung cancer, with prognostic implications for early-stage disease. Lung Cancer. Elsevier; 2018 Oct 2;125:174–84.
22. Yan Z, Jiang J, Li F, Yang W, Xie G, Zhou C, et al. Adenovirus-mediated LRIG1 expression enhances the chemosensitivity of bladder cancer cells to cisplatin. Oncol Rep. 2015 Apr;33(4):1791–8.
23. Wang X, Xiao Q, Xing X, Tian C, Zhang H, Ye F, et al. LRIG1 enhances cisplatin sensitivity of glioma cell lines. Oncol Res. 2012;20(5-6):205–11.
24. Wu X, Hedman H, Bergqvist M, Bergström S, Henriksson R, Gullbo J, et al. Expression of EGFR and LRIG proteins in oesophageal carcinoma with emphasis on patient survival and cellular chemosensitivity. Acta Oncol. 2012 Jan;51(1):69–76.
25. Stutz MA, Shattuck DL, Laederich MB, Carraway KL, Sweeney C. LRIG1 negatively regulates the oncogenic EGF receptor mutant EGFRvIII. Oncogene. 2008 Jun 9;27(43):5741–52.
26. Fidler IJ. The pathogenesis of cancer metastasis: the “seed and soil” hypothesis revisited. Nat Rev Cancer. 2003 Jun;3(6):453–8.
27. Valastyan S, Weinberg RA. Tumor Metastasis: Molecular Insights and Evolving Paradigms. Cell. Elsevier Inc; 2011 Oct 14;147(2):275–92.
28. Lambert AW, Pattabiraman DR, Weinberg RA. Emerging Biological Principles of Metastasis. Cell. Elsevier Inc; 2017 Feb 9;168(4):670–91.
29. Yokdang N, Hatakeyama J, Wald JH, Simion C, Tellez JD, Chang DZ, et al. LRIG1 opposes epithelial-to-mesenchymal transition and inhibits invasion of basal-like breast cancer cells. Oncogene. Nature Publishing Group; 2016 Jun 2;35(22):2932–47.

30. Torigoe H, Yamamoto H, Sakaguchi M, Youyi C, Namba K, Sato H, et al. Tumor-suppressive effect of LRIG1, a negative regulator of ErbB, in non-small cell lung cancer harboring mutant EGFR. Carcinogenesis. 2018 Mar 13;65:87–9.
31. Mao F, Holmlund C, Faraz M, Wang W, Bergenheim T, Kvarnbrink S, et al. Lrig1 is a haploinsufficient tumor suppressor gene in malignant glioma. Oncogenesis. 2018 Feb 2;7(2):13.
32. Zhang SZ, Lipsky MM, Trump BF, Hsu IC. Neutral red (NR) assay for cell viability and xenobiotic-induced cytotoxicity in primary cultures of human and rat hepatocytes. Cell Biol Toxicol. Kluwer Academic Publishers; 1990 Apr;6(2):219–34.
33. Hafner M, Niepel M, Chung M, Sorger PK. Growth rate inhibition metrics correct for confounders in measuring sensitivity to cancer drugs. Nature Methods. 2016 May 2;13(6):521–7.
34. Schneider C, Rasband WS, Eliceiri KW. NIH Image to ImageJ: 25 years of image analysis. Nature Methods. 2012 Jul 1;Jul;9(7):671–5.
35. Jamovi [Internet]. 1st ed. The Jamovi Project. Available from: https://jamovi.org
36. R: A language and environment for statistical computing [Internet]. 3rd ed. R Core Team. Available from: https://cran.r-project.org
37. Zhang X, Song Q, Wei C, Qu J. LRIG1 inhibits hypoxia-induced vasculogenic mimicry formation via suppression of the EGFR/PI3K/AKT pathway and epithelial-to-mesenchymal transition in human glioma SHG-44 cells. Cell Stress Chaperones. 2015 Jul;20(4):631–41.
38. Li W, Zhou Y. LRIG1 acts as a critical regulator of melanoma cell invasion, migration, and vasculogenic mimicry upon hypoxia by regulating EGFR/ERK-triggered epithelial-mesenchymal transition. Biosci Rep. 2019 Jan 31;39(1).
39. Yang J-A, Liu B-H, Shao L-M, Guo Z-T, Yang Q, Wu L-Q, et al. LRIG1 enhances the radiosensitivity of radioresistant human glioblastoma U251 cells via attenuation of the EGFR/Akt signaling pathway. Int J Clin Exp Pathol. 2015;8(4):3580–90.
40. Hoffman RM. Metastatic Orthotopic Mouse Models of Lung Cancer. In: Driscoll B, editor. Lung Cancer: Volume 1: Molecular Pathology Methods and Reviews. Totowa, NJ: Humana Press; 2003. pp. 457–64. (Lung Cancer: Volume 1: Molecular Pathology Methods and Reviews).

Figures

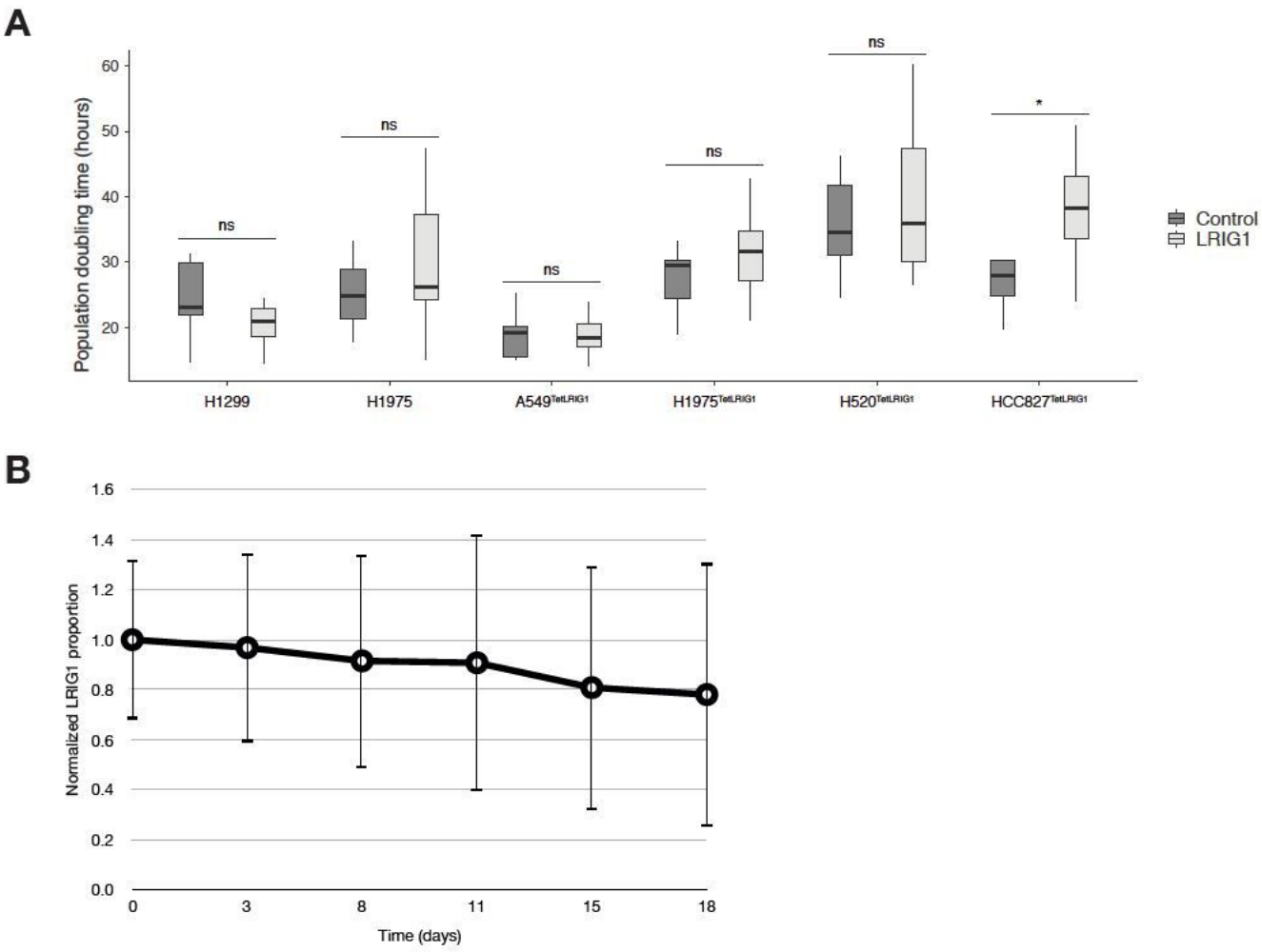

Figure 1

LRIG1 does not affect cell proliferation rates of most NSCLC cell lines. (A) Proliferation rates of NSCLC cell lines without or with LRIG1 overexpression. Different NSCLC cell lines were transduced with a constitutive LRIG1 expression vector (H1299 and H1975) or an inducible LRIG1 expression vector

(A549TetLRIG1, H1975TetLRIG1, H520TetLRIG1, and HCC827TetLRIG1). The inducible cell lines were either not treated (control) or treated with doxycycline (LRIG1) to induce LRIG1 expression. Cell proliferation was monitored via live-cell imaging using a Holomonitor M4 instrument. Shown are the calculated population doubling times, in hours, for the respective cell lines. For the doxycycline-inducible cell lines, data are shown both for untreated cells and doxycycline-treated cells. Shown are box plots; means are from 10 areas measured over 48 hours with 1 time point per hour, in 3 technical replicates and, for H1299 and H1975, 4 biological replicates. Significance is represented using * for $p < 0.05$. (B) Competitive proliferation assay. The relative proliferation rates were compared between H1299 control cell populations and LRIG1-overexpressing H1299 cell populations by co-culturing the cell populations and determining the ratio between the control and LRIG1-overexpressing populations at predefined time points using ddPCR. Shown is a curve of changes in the ratio over 18 days. Error bars represent SD. Means and SD are from 3 experiments.

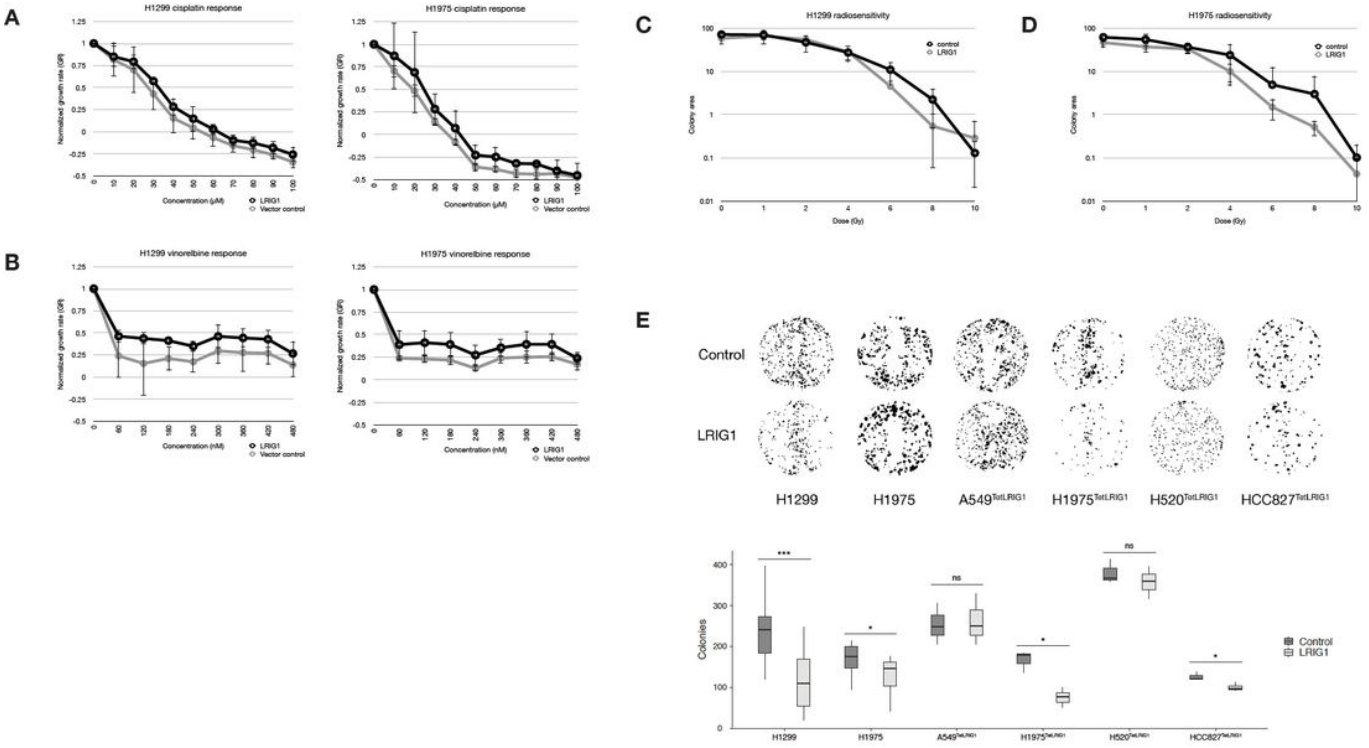

Figure 2

LRIG1 does not significantly affect chemosensitivity or radiosensitivity in the H1299 and H1975 cell lines. (A) Cisplatin sensitivity. The NSCLC cell lines H1299 and H1975 were transduced with a constitutive LRIG1 expression vector or an empty control vector, then treated with different concentrations of cisplatin. Cell viability was measured using resazurin reduction, and a normalized growth rate (GR) was calculated with untreated cells as reference. Shown is a dose-response GR curve, with 1.0 representing untreated cells. Means were calculated from 3 technical replicates and 4 biological replicates per cell line variant. (B) Vinorelbine sensitivity. H1299 and H1975 cells with a constitutive LRIG1 expression vector or an empty control vector were treated with vinorelbine and analyzed using the same methods as above. (C) Radiosensitivity in H1299 cells. Cells transduced with a constitutive LRIG1 expression vector or control vector were irradiated and plated to determine clonogenicity. Shown is a dose-response curve showing colony area for each radiation dose. Means were calculated from 3 technical replicates and 4 biological replicates per cell line variant. (D) Radiosensitivity in H1975 cells. Cells transduced with a constitutive LRIG1 expression vector or control vector were irradiated, plated, and analyzed using the same methods as above. (E) Colony-forming ability in untreated cells. NSCLC cell lines were transduced with a constitutive LRIG1 expression vector (H1299 and H1975) or an inducible LRIG1 expression vector (A549TetLRIG1, H1975TetLRIG1, H520TetLRIG1, and HCC827TetLRIG1). The inducible cell lines were either not treated (control) or treated with doxycycline (LRIG1) to induce LRIG1 expression. Shown are examples of stained colonies (above) and a box plot showing the number of colonies for each cell line (below). Means were calculated from triplicates in 3 experiments. Significances are represented using * for $p < 0.05$ and *** for $p < 0.001$.

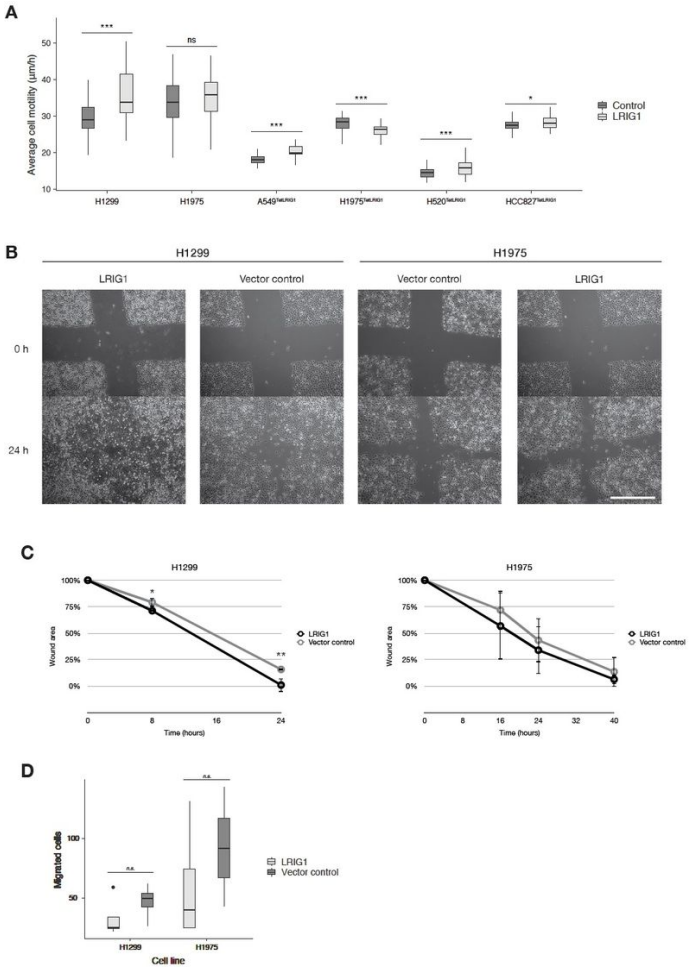

Figure 3

LRIG1 increased the wound healing and migration rates in H1299 but had minor effects on other cell lines. (A) Single cell migration rates. A panel of NSCLC cell lines transduced with a constitutive LRIG1 expression vector (H1299 and H1975) or an inducible vector (A549TetLRIG1, H1975TetLRIG1, H520TetLRIG1, and HCC827TetLRIG1) were sparsely seeded onto 24-well plates and monitored using a HoloMonitor M4 microscope. The inducible cells were either not treated (control) or treated with doxycycline to induce LRIG1 expression (LRIG1), Migration rates were measured on a population level per area imaged. Shown are box plots with means from 10 imaged areas per cell line over 48 hours, with 360 measurements per area, in triplicates. Significances are represented using * for $p < 0.05$ and *** for $p < 0.001$. (B) Wound healing assay. The wound closure rate was compared between LRIG1-overexpressing and vector control transduced H1299 or H1975 cells. Shown are timelapse phase contrast images of wound closure in near confluent monolayers. The scale bar is 100 µm. (C) Quantification of the assays shown in B. Wound areas are represented in percentages of the initial area at t = 0. Significances are represented using * for $p < 0.05$ and ** for $p < 0.01$. (D) In vitro migration using the transwell assay. The NSCLC cell lines H1299 and H1975 were transduced with a constitutive LRIG1 expression vector or an empty control vector, then serum-starved overnight, seeded into the inner chamber of transwell inserts, and incubated for 8 hours. Shown are box plots of the average amount of migrated cells. Means were calculated from 3 technical replicates and 4 biological replicates per cell line variant. Significances are represented using * for $p < 0.05$.

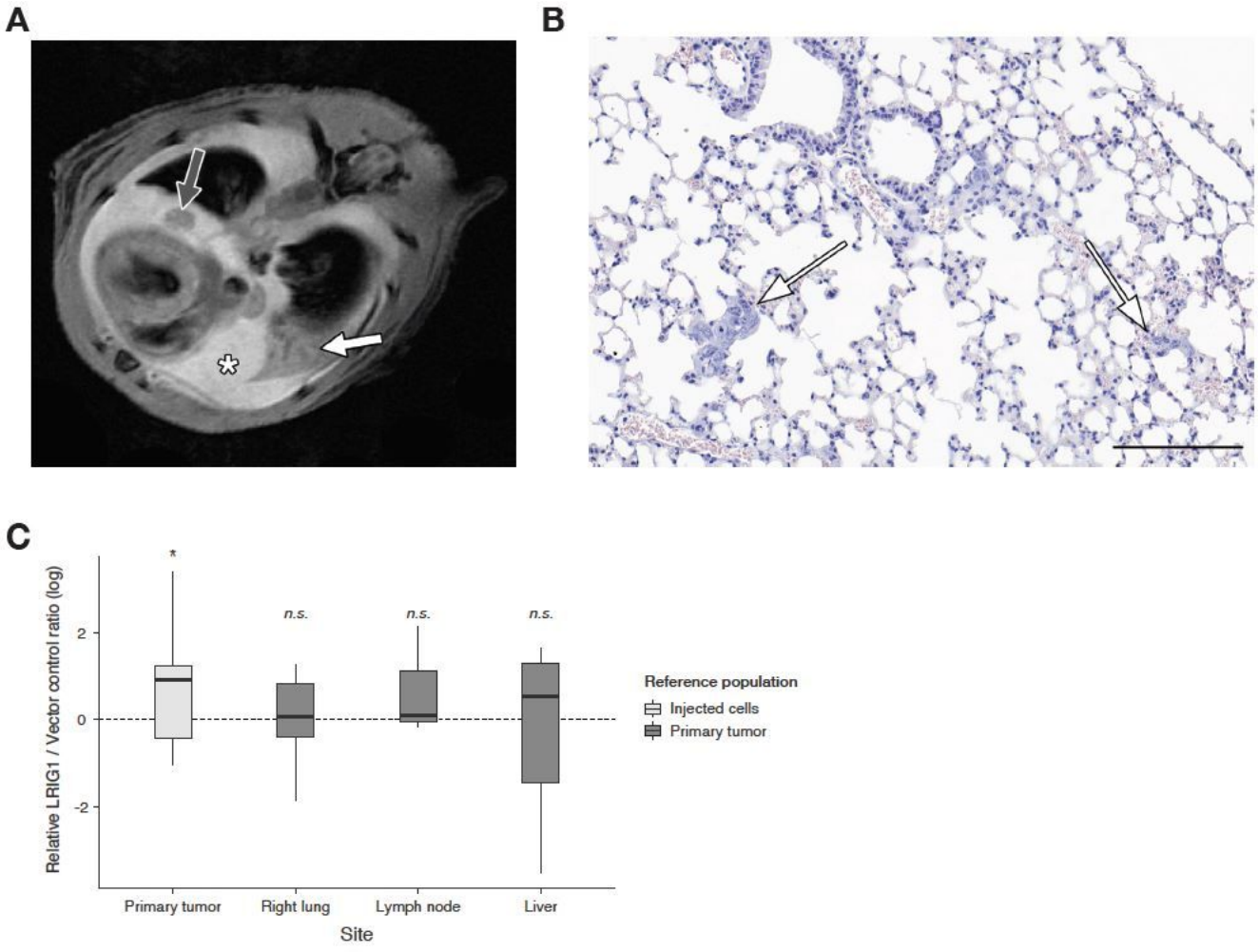

Figure 4

LRIG1 was neither enriched nor depleted, in H1299 hematogenous metastases. (A) Primary tumor with locoregional spread. CIEA NOG mice were orthotopically injected in the left lung with the NSCLC cell line H1299. Shown is a T1 FLASH MRI image of a mid-axial section of a symptomatic, tumor-bearing mouse. The white arrow indicates a primary tumor in the left lung. The asterisk denotes pleural effusion. The grey arrow indicates pathologically enlarged mediastinal lymph nodes. (B) Morphology of micrometastases. Only H1299 formed intraparenchymal metastases in the right lung. Shown is a section from a contralateral lung from a mouse injected with H1299 cells. Intraparenchymal micrometastases are indicated by arrows. The scale bar is 100 µm. (C) Cell populations in H1299 primary tumors and metastatic sites. CIEA NOG mice were injected with a mixed population of H1299 cells transduced with a constitutive LRIG1 expression vector and H1299 cells transduced with an empty vector, both co-expressing either ZsGreen1 or mCherry. The ratio of LRIG1 copies to vector controls was measured by ddPCR on DNA extracted from tissues. For each primary tumor, the ratio was normalized against the measured ratio in saved samples of the corresponding cell suspension. For metastatic sites, the ratio was normalized against the corresponding primary tumor. Shown are box plots of LRIG1-to-control-vector ratios, measured in triplicates across 22 mice. Significances are represented using * for $p < 0.05$.

Supplementary Files

This is a list of supplementary files associated with this preprint. Click to download.

- figS1.pdf
- ColonyCounter.ijm
- Uncroppedblots.tif
- ScratchAssay.ijm
- SupplementalTables.docx